HiSST: International Conference on
High-Speed Vehicle Science Technology
26–29 November 2018, Moscow, Russia

Flow Visualization and Control of Unstarting Scramjet Inlet-Isolator

Kyungrae Kang[1], Lydia Wermer[2], Jong Ho Choi[3], Seung Jin Song[4], Seong-kyun Im[5] and Hyungrok Do[6]

Abstract

Shock-compressed flows in a model scramjet isolator were visualized using a high-speed schlieren imaging system to reveal unstarting and boundary layer suction-controlled flow behaviors. The model scramjet having a rectangular cross-section and contraction ratio of 4 at the inlet was tested in Mach 6 freestream flows. Inlet unstart, seen as flow spillage at the inlet caused by downstream flow choking, was triggered by high-pressure nitrogen jet injection after the isolator that simulates excessive heat release and resulting pressure rise in the combustor. Transient movements of an upstream-propagating shockwave, referred to as the unstart shock, and its fluctuation behavior upstream of the inlet are temporally resolved. Boundary layer suction was applied in the isolator wall removing a small portion (~2%) of the isolator flow from the boundary layer when activated. It is shown that the unstart shock, which completes the unstart process when arriving at the inlet, can be held or decelerated in the isolator depending on the suction activation time: early activation can stop while late activation can delay the unstart.

Keywords: scramjet, inlet unstart, schlieren, active flow control

Nomenclature

CR – Contraction ratio
Ma – Mach number
J – Jet momentum ratio
AoA – Angle of Attack

Subscripts
0 – stagnation(total) property
f – freestream
j – jet

1. Introduction

A scramjet is an air-breathing propulsion system developed for hypersonic flights. Unlike other conventional propulsion systems which burn fuel in subsonic flows, a scramjet is designed to burn fuel supersonically so that the flow inside the engine is supersonic throughout. The supersonic compressible internal flows in scramjets inherently accompany complex flow dynamics of turbulence, shockwaves, shockwave-boundary layer interactions (SBLI), and flow choking under certain unintended flow conditions. Notably, flow choking can cause inlet unstart which dramatically reduces the thrust of the engine.

[1] *Seoul National University, Seoul, Republic of Korea, krkang@snu.ac.kr*
[2] *University of Notre Dame, Notre Dame, IN, 46556, USA, lwermer@nd.edu*
[3] *Agency for Defense Development, Daejeon, Republic of Korea, cjh0322@add.re.kr*
[4] *Seoul National University, Seoul, Republic of Korea, sjsong@snu.ac.kr*
[5] *University of Notre Dame, Notre Dame, IN, 46556, USA, sim@nd.edu*
[6] *Seoul National University, Seoul, Republic of Korea, hyungrok@snu.ac.kr*

Inlet unstart in scramjets can be triggered by a sudden back pressure rise, excessive fuel injection, and freestream turbulence-enhanced boundary layer thickening/separation that can induce flow choking [1~7]. The mass flow rate of the scramjet internal flow when choked, that is the maximum allowable flow rate, strongly depends on gas conditions including stagnation pressure, gas density, flight altitude, flight Mach number, inlet-isolator-combustor geometry, bank angle, and angle of attack. In general, the inlet will unstart when the captured inlet mass flow rate exceeds the maximum allowable flow rate under the choked condition. In short, when the scramjet internal flow is choked for some reason, the flow rate will be limited so that the rest of the captured air will be spilled at the inlet or a shockwave appearing later in front of the inlet will limit the flow rate beforehand [6~10]. This shockwave at the forefront of the vehicle is unstable, asymmetric along the flight trajectory, and abruptly increases drag on the vehicle. Furthermore, loss of the intake air, which is the major combustion energy carrier to produce thrust, will result in the loss of thrust [1, 6, 8~10].

The most effective way of suppressing or preventing inlet unstart is to control the fuel injection rate properly which affects both the downstream mass addition and combustion heat release. However, changing fuelling rate often takes much longer than the unstart process. In addition, the fuel injection rate generally needs to be reduced to stop the unstart process, which would decrease the thrust. Therefore, supplemental unstart control strategies that can have a quick response time and minimize the thrust loss are required. For example, propagation of the unstart shockwave could be delayed to save time for the fuel injection control to be effective, or effective internal flow area can be enlarged by suppressing boundary layers or their separation which could result in the increase of the maximum allowable mass flow rate through the engine.

For supplemental control purposes, active and passive flow control methods have been proposed and tested [11~18]. Passive surface devices such as micro-ramps and vortex generators [11~13] were used to redistribute the kinetic energy of the fluid or to alter the shockwave-boundary layer interactions so that the mass flow rate of the choked flow can be increased. One active flow control strategy is mass extraction from the internal flow which would immediately lessen mass loading and is potentially capable of preventing inlet unstart caused by the limited mass flow rate from choking. However, mass extraction could be costly as the inflow rates, the freestream flow rate and the fuel flow rate, directly affect the thrust. Another strategy is to control the boundary layer of supersonic flows to increase the choked flow rate with zero or minimal mass extraction. The sudden growth of the boundary layer due to the downstream pressure rise can induce a leading shockwave, the unstart shockwave, to move upstream. Therefore, reducing the boundary layer thickness can effectively delay or stop the unstart process by enlarging the effective internal flow area and decreasing the stagnation pressure loss to increase the limit of choked flow rate. A dielectric barrier discharge (DBD) actuator can suppress the boundary layer by directly adding momentum into the boundary layer flows, but without mass extraction as it acts as a vortex generator [14]. However, it requires a high-voltage power supply on board and surface electrodes that are vulnerable to contamination making DBD actuators less desirable in real applications. Instead, boundary layer bleeding has been the most popular strategy for suppressing unstart as it extracts a tiny amount of mass, typically a few percents or less of the freestream mass flow rate so that the loss in thrust can be minimized [19]. A number of experimental and numerical studies have confirmed that boundary layer bleeding can effectively suppress the growth of boundary layer or even local separation to stop inlet unstart and extend engine operability under a range of flow conditions [15~18].

Previous studies on boundary layer suction-control in scramjets often used suction holes or slots in a narrow surface area at an upstream location or near the inlet to suppress early boundary layer developments [15~18]. This is particularly effective in increasing core flow area and controlling shock trains in an isolator. On the other hand, the primary target of this study is to stop the unstart process beginning at a downstream location, therefore, the suction holes also need to be placed downstream. For this reason, the suction holes are machined on an isolator wall and are broadly distributed to hold and impede the unstart shock while it propagates upstream through the isolator.

2. Experimental Setup

2.1. Test model scramjet

A schematic view of the model scramjet used in this study consisting of an inlet, isolator, combustor, and divergent exhaust is shown in Fig. 1. The inlet has a compression ramp on its upper lip where the ramp angle, α, is 12°. The lower lip of the inlet is recessed horizontally by 55 mm from the upper lip location to provide better starting characteristics, i.e., thinner boundary layer at the lower side. The isolator and the combustor have a rectangular and constant cross-section of 32 mm (width) by 11 mm (height). The combustor has a diverging fuel jet nozzle whose circular throat has a diameter of 1.5 mm. The nozzle is inclined toward downstream, 60° upward from the lower combustor wall plane. A wall cavity flameholder is carved 100 mm downstream from the jet injection location, which extends 12 mm downstream from the cavity leading edge (back-facing vertical step of 3 mm depth) with a linearly inclined close-up ramp. The model scramjet is installed upside-down in the test section for convenient tubing of the fuel jet supply line and suction-hole connections

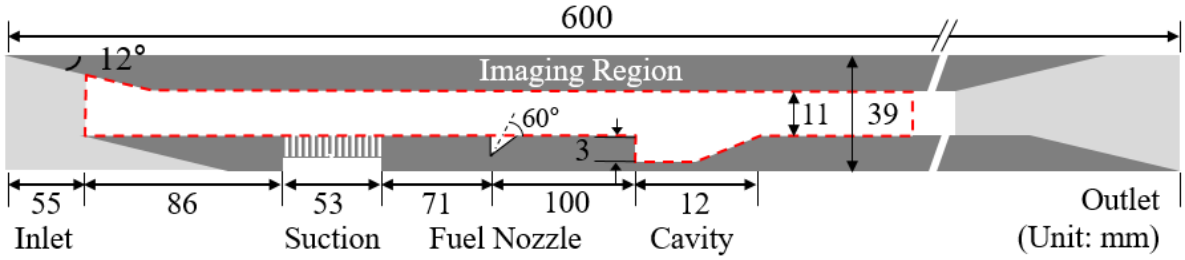

Fig. 1 Schematic of the model scramjet

The suction holes are on the lower wall of the isolator being uniformly distributed between 124 mm and 71 mm upstream from the fuel jet injection nozzle. 78 holes of 0.8 mm in diameter are drilled in the area evenly separated by 4 mm, 6 rows and 13 columns along the stream-wise direction as shown in Fig. 2. The hole diameter is chosen for minimal flow disturbance and convenience in machining.

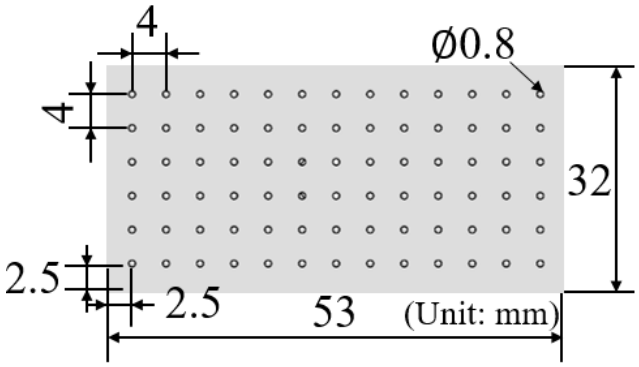

Fig. 2 Configuration of the perforated plate installed for boundary layer suction

2.2. Test Facility and experimental setup

A supersonic wind tunnel, ACT-1 at the University of Notre Dame, is used for the experimental investigation. ACT-1 is a blow-down wind tunnel capable of generating high enthalpy supersonic and hypersonic flows with a one second test time. Note that the arc-heater of the tunnel is not used in this

study as the aim of this study is characterizing unstarting flows induced by mass addition which is achieved by high-pressure nitrogen jet injection. Therefore, room temperature compressed nitrogen balanced with 20% carbon dioxide (298K) is accelerated through a converging/diverging (C/D) nozzle providing uniform supersonic flows in the test section for approximately 0.5 seconds. The model scramjet is installed near the exit plane of the C/D nozzle. The test section is connected to a vacuum tank of roughly 10 m^3 and a two-stage high-performance vacuum pump, keeping the ambient pressure below 20 Pa prior to running. More detailed tunnel information is presented in [10, 20].
An additional small vacuum chamber of 2.25 liter, that is evacuated prior to the tunnel operation, is connected to the suction holes to drive the suction flow from the boundary layer on the isolator to the chamber. The opening of the connection between the suction holes and the vacuum chamber is controlled by a fast-acting solenoid valve (SMC, VT307). In addition, a high-temperature ultra-miniature pressure transducer (Kulite XCE-062-5A) is attached on the passage of the suction flow to monitor the flow pressure traces at a sampling frequency of 20kHz for estimating the suction flow rate.
Room temperature high-pressure nitrogen was injected through the fuel jet nozzle to trigger the mass-loading-induced inlet unstart. The nitrogen jet is injected for 400 ms beginning at 10 ms after the freestream. The nitrogen jet injection is controlled by a pressure regulator on the pressurized nitrogen tank and a fast-acting solenoid valve (SMC, VT317). A heavy duty pressure transducer (Honeywell PX2) is chosen for monitoring the nitrogen jet pressure, which works at up to 150 psi with an accuracy of 0.375% (±0.25% of the full scale).

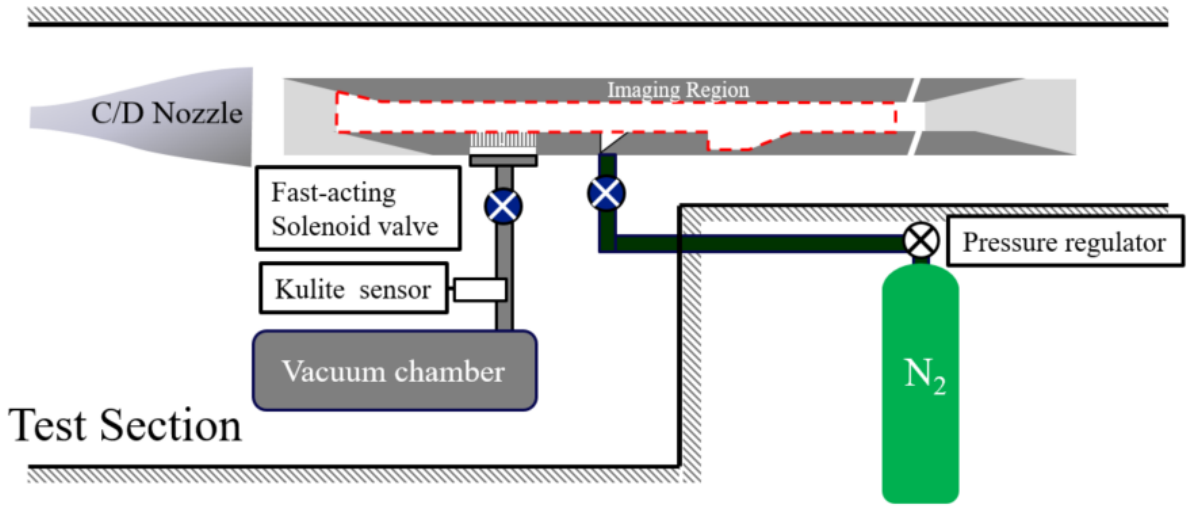

Fig. 3 Schematic of experimental setup

To visualize the transient unstarting flow, high-speed schlieren imaging technique is utilized. A schematic of the optical setup is presented in Fig. 4. High-speed diode laser (Cavitar Cavilux Smart) of 640 nm wavelength is used as the light source. One collecting, two collimating and two focusing lenses are aligned to redirect the laser beam that projects the density field in and around the model scramjet on the high-speed camera sensor (Photron, FASTCAM Ultima APX). A knife-edge is placed in a horizontal position and the fast-framing camera records instantaneous schlieren images at 4,000 fps rate to capture the transient behaviors of the unstarting flows. Since the region of interest (ROI) to be imaged is broad in horizontal direction (length of the model scramjet is 600 mm), the ROI is divided into five section horizontally (one section covers the inlet and the rest are in the isolator and combustor) to be imaged in separate tunnel runs moving the schlieren setup back and forth under a fixed experimental condition.

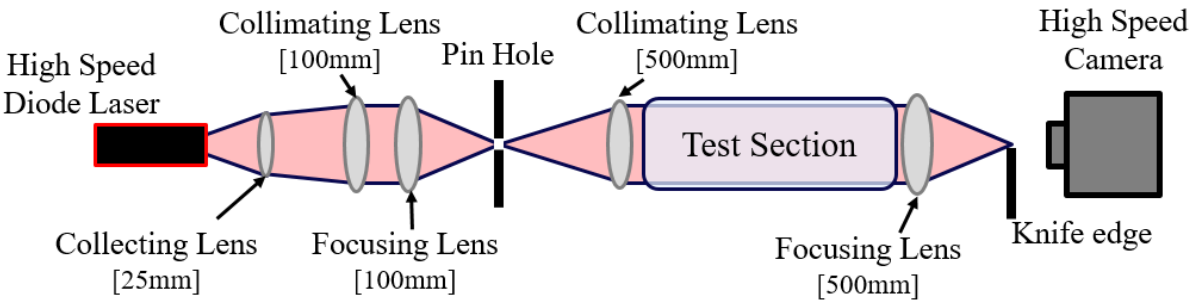

Fig. 4 Schematic of the schlieren setup

2.3. Test matrix

Three different experimental conditions are tested as shown in Table 1. Freestream Mach number, freestream stagnation pressure, and nitrogen jet injection pressure are kept unchanged in all test cases at 6, 3 bars, and 5.6 bars, respectively. Note that the jet pressure is time-averaged pressure over the injection period. Case 1 being the reference case without the suction control, the boundary layer suction in Cases 2 and 3 are activated 10 ms and 20 ms after the triggering of the nitrogen jet injection, respectively.

Table 1. Text matrix for inlet unstart study

Case #	*Ma*	P_{0f} [bar]	P_{0j} [bar]	*Suction Delay [ms]*
1	6	3	5.6	None
2	6	3	5.6	+10
3	6	3	5.6	+20

3. Result

3.1. Case 1: Unstarting flow without boundary-layer suction

Figure 5 shows the schlieren-imaged flow structures in the isolator and combustor before and after the inlet unstart. The black rectangle in the middle of the image is due to a pillar in the tunnel blocking the light source. Compressible flow features such as shockwaves, expansion fans, a supersonic shear layer above the cavity flameholder, and fine wrinkles from non-uniform pressure fluctuations are clearly resolved prior to the unstart (Fig. 5(a)). This is because the internal flow in the model scramjet is supersonic and compressible being disturbed by the compression ramp at the inlet, a nitrogen jet, and a cavity flameholder to induce strong density gradient field that can be readily imaged by the schlieren imaging technique. Nevertheless, these high-contrast flow features in schlieren images disappear once the scramjet flow is unstarted because the unstarted flow is subsonic where non-uniform pressure field, if any, would be quickly flattened out by pressure waves. As shown in previous studies [6, 20, 21], strong shockwaves anchored in front of unstarted inlets reduce inlet-captured air flow rate and decelerate the scramjet internal flow to be subsonic throughout the isolator and combustor.

To simulate unstart situations in scramjets by choking, a high-pressure nitrogen jet is injected to raise the mass flow rate until the internal flow is choked at a downstream location. When the flow is choked and the flow rate is limited at the choked location, the internal flow channel, e.g., the isolator and combustor, cannot fully handle the inlet-captured flow rate. In other words, the inflow rate (i.e., intake and jet flow rate) will exceed the outflow rate (i.e., maximum allowable flow rate or choked flow rate), thus, the rest of the inflow exceeding the choked flow rate will be accumulated in the channel to

continuously raise the downstream pressure and to extend the high-pressure region further upstream. This will be seen as the rapid growth or separation of boundary layers. As the thickened boundary layer, which is induced by high back pressure from the nitrogen jet, moves further upstream where the flow is faster in supersonic regime, a shock system will appear and propagate upstream to extend the subsonic high-pressure region toward the inlet. This unsteady shock system has been referred to as the unstart shock. And the transient flow where the unstart shockwave propagates upstream to disgorge the shockwave system out of the inlet is often referred to as unstarting flows. When the unstart shock arrives at the inlet, the incoming flow will be spilled at the inlet and an unsteady shockwave staying upstream of the inlet will be induced. The inlet flow spillage and formation of the upstream shockwave will immediately reduce the inflow rate to balance with the choked flow rate. In short, the inlet unstart is simply to match the inflow rate with the outflow rate through the scramjet when the internal flow is choked.

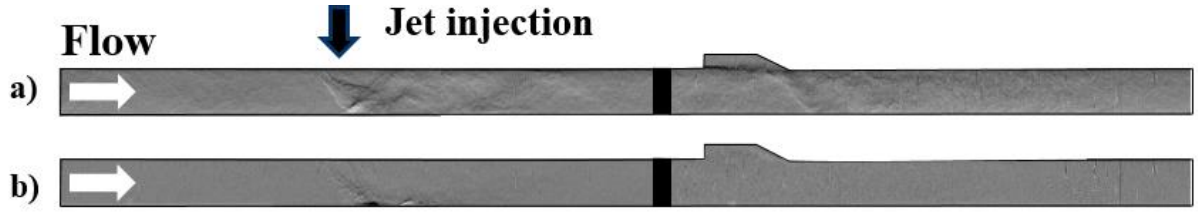

Fig. 5 Flow field a) before unstart b) after unstart

Fig. 6 illustrates clear differences in the inlet flow structures before and in the process of the inlet unstart. In Fig. 6(a), under a normal inlet flow condition, the incident shockwave induced by the inlet compression ramp (upper lip of the inlet, however, on the bottom in the image) and the Mach wave induced by the cowl (lower lip of the inlet) are clearly visualized; recall that the model scramjet is installed upside down in the test section. On the other hand, the inlet flow is unsteady and non-uniform (Fig. 6(b)) since the unsteady unstart shock has arrived at the inlet.

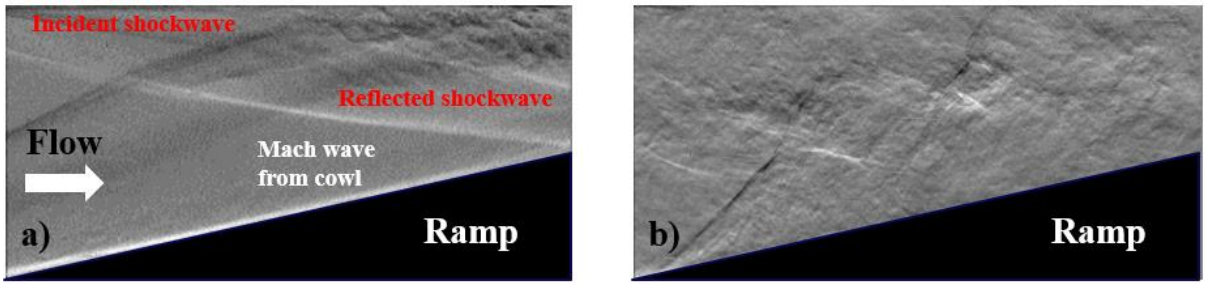

Fig. 6 Comparison between a) started inlet and b) unstarted inlet

The unsteady inlet flow structure indicates nearing the completion of the inlet unstart process, which is preceded by upstream propagation of an unstart shock as illustrated in Fig. 7. The time labels on the right of the images are the time delays from the beginning of the tunnel run, and the red arrows highlight the location of the unstart shock at each time instance. The unstart shock first appears later than 25 ms but before 50 ms at a location downstream of the cavity flameholder. Around the cavity holder the unstart shockwave propagates upstream relatively fast (approximately 6m/s). Approaching the nitrogen jet the unstart shock propagates in a much slower speed (approximately 2m/s), and the propagation is further decelerated (approximately 0.5m/s) after passing by the jet location, taking a much longer time in reaching the inlet (at approximately 300 ms).

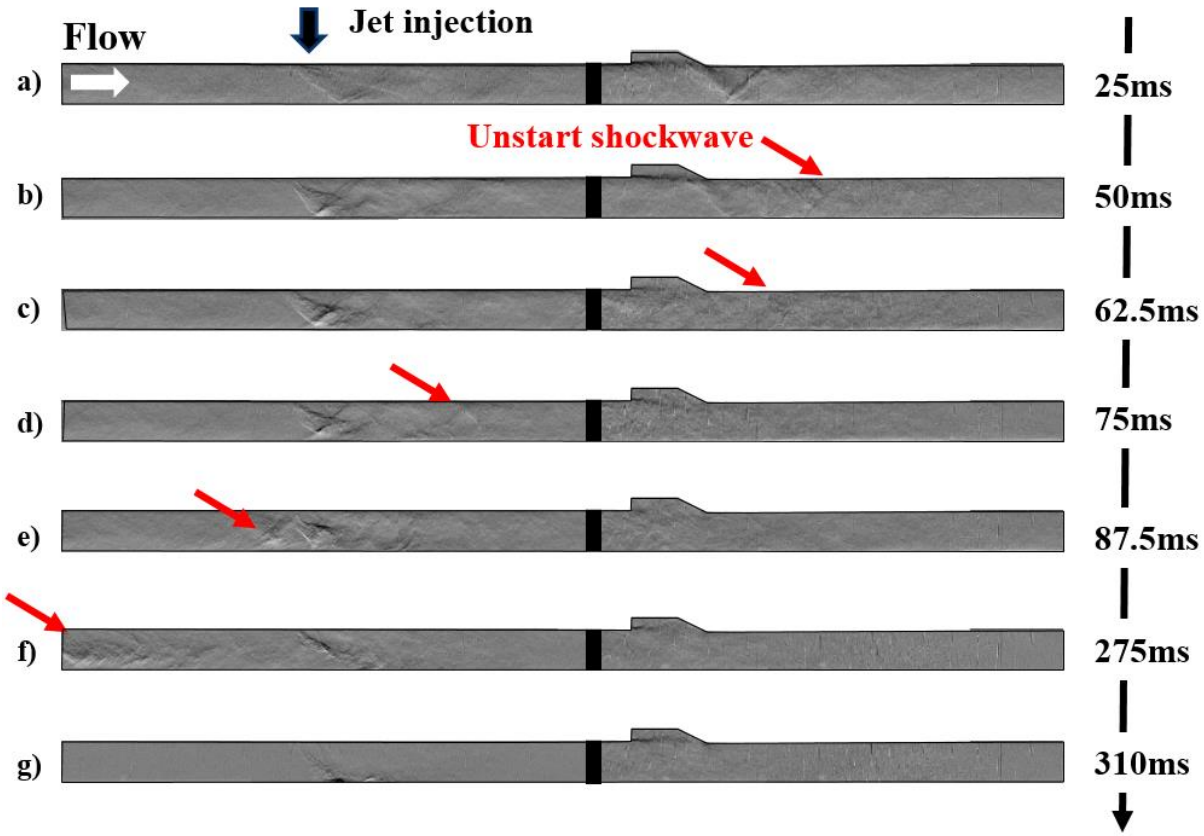

Fig. 7 Overview of unstart shockwave propagation

Presumably, the unstart shock dynamics are strongly dependent on the pressure distribution in the scramjet internal flow channel [6, 21, 22]. Therefore, the propagation behavior along the model scramjet of varying spatial pressure distribution has been analyzed in this study and is described in detail through Fig. 8 – 11. The figures are time-sequential schlieren images near the cavity, around the jet injection location, in the isolator, and at the inlet, respectively. Recall that the region of interest from the inlet to the combustor exit are divided into 5 imaging sections, and four downstream sections except for the one imaging the inlet cover the isolator and combustor; Figs 5 and 7 are concatenated images of the four downstream sections. The reference time of each figure is the time instance when the first image is taken just before the unstart shock arrives in the imaging section.

Figure 8 presents time-sequential schlieren images taken while the unstart shock passes through the imaging section near the cavity flameholder. The unstart shock first appears in the imaging section in Fig. 8(b) and leaves roughly 15 ms later (Fig. 8(e)). Since the high-pressure nitrogen jet is injected upstream of the cavity and the flow chokes further downstream of the imaging section, no significant local pressure gradient hindering the unstart shock propagation is present while the cavity flameholder induces locally non-uniform pressure field above it. At downstream of the cavity, there exists a series of reflected shockwaves originated from the inclined close-up ramp of the cavity. Therefore, the flow just upstream of unstart shockwave has a higher stagnation pressure and a larger effective area as it moves upstream which, in turn, leads to increased choked mass flow rate. As a result, unstart shockwave is relatively slower as the choked mass flow rate keeps increasing as unstart shock moves upstream, as shown in Fig. 8(b) to (c). Furthermore, depending on the static pressure gradient that the unstart shockwave experiences, the propagation speed of unstart shockwave can differ. When unstart shockwave is under a favorable pressure gradient, the pressure rise across the shockwave should decrease as it moves upstream. Therefore, the unstart shockwave must see the flow at a decreased speed, that is, unstart shockwave must decelerate under a favorable pressure gradient and vice versa. Flows near the cavity clearly show this acceleration or deceleration of unstart shockwave propagation under different pressure gradients.

The shockwave generated by the inclined close-up ramp of the cavity locally induces favorable pressure gradient behind, i.e., decreasing pressure toward downstream. Therefore, unstart shockwave is

relatively slower as shown in Fig. 8(b) to (c). Flow inside the cavity is under an adverse pressure gradient from the ramp shockwave and the separation at the backward-facing step. Therefore, unstart shockwave is significantly faster (approximately 6 times as faster as in Fig. 8(b) to (c)) and almost immediately reaches the upstream portion of the cavity, as shown in Fig. 8(c) to (d). Having overcome the local expansion from the backward-facing step, the unstart shockwave encounters a small or almost zero pressure gradient through the isolator and hence is accelerated again. After unstart shockwave passes the cavity, the supersonic shear layer at the corner of the backward-facing step significantly weakens, which indicates that the Mach number of the flow is reduced due to unstart shockwave.

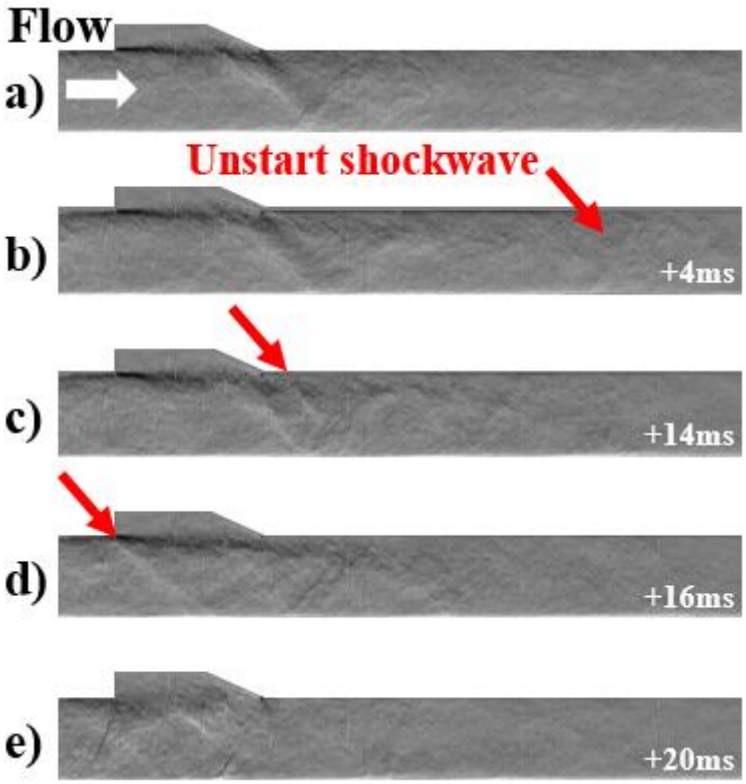

Fig. 8 Unstart shockwave propagation near the cavity

Figure 9 describes the unstart shock propagation behavior near the high-pressure nitrogen jet injection location. The high-pressure jet carries an abnormally large amount of mass to be injected into the scramjet internal flow for triggering the inlet unstart initiated by downstream flow choking. Therefore, the high-momentum jet induces a strong shockwave that hits the opposite wall. This jet-induced shockwave bounces up and down to produce a train of oblique shockwaves behind the jet (see Fig. 9(a)). These shockwaves elevate the static pressure of the flow, however, reducing the stagnation pressure and the flow speed due to the shock-induced compression. Consequently, as the unstart shock moves further upstream, it will encounter faster flows of higher stagnation pressure that contains the jet-supplied high-pressure nitrogen and the inlet-captured air. The unstart shock is an upstream-propagating compression wave driven by the downstream pressure build-up from gradual mass accumulation. Therefore, the unstart shockwave propagation would be decelerated since the propagation needs higher and higher mass accumulation as it moves toward upstream due to higher stagnation pressure, as discussed earlier in Fig. 8(b) to (c). This is coincident with the observation in Fig. 9. It is found that the shock propagation gets significantly slower as it approaches the jet, e.g., approximately 21 ms is taken to reach the middle of the imaging section near the jet while the shock passes through the whole imaging section within about 15 ms in a further downstream region around the cavity. Later the unstart shock system merges and overlaps with the resident supersonic jet and the jet-induced shockwave structures as shown in Figs. 9(c) and 9(d). After the unstart shock passes the jet region seen in Fig. 9(e), the jet-induced shockwaves and the flow structure become completely different because Mach number of the approaching flow is significantly reduced behind the unstart shockwave.

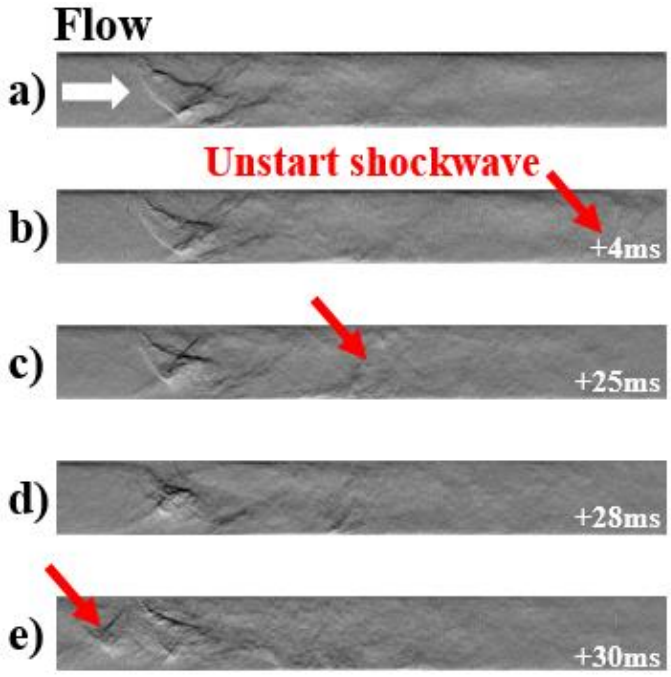

Fig. 9 Unstart shockwave propagation near jet

In the isolator which is upstream of the nitrogen jet injection location, the incident shockwave from the inlet induces a train of shockwaves, therefore, the unstart shock propagation would be decelerated again as discussed earlier. Considering that the incident shockwave is the strongest, one can expect rapid deceleration as the unstart shock approaches the inlet region as the incremental stagnation pressure rise will be the greatest as unstart shock moves upstream. In Fig. 10, the unstart shock system resides in the imaging section for over 200 ms. At 150 ms, the unstart shockwave reaches the end of the imaging region of the isolator. After reaching the first shockwave-impingement location where the boundary layer separates and reattaches right after as illustrated in Fig. 10(k), the unstart shock interacts with the incident shock to expand the separation region and eventually two separation regions, from the incident shock and from the unstart shock, merge into one (Fig. 10(l)). As time goes on, due to the unbalance between the inflow and outflow rate (the inflow rate, intake air + nitrogen jet, is still greater than the choked flow rate), the downstream pressure will gradually increase from the mass accumulation as mentioned earlier, and the unstart shock will eventually overcome the strongest incident shockwave to be disgorged out the inlet.

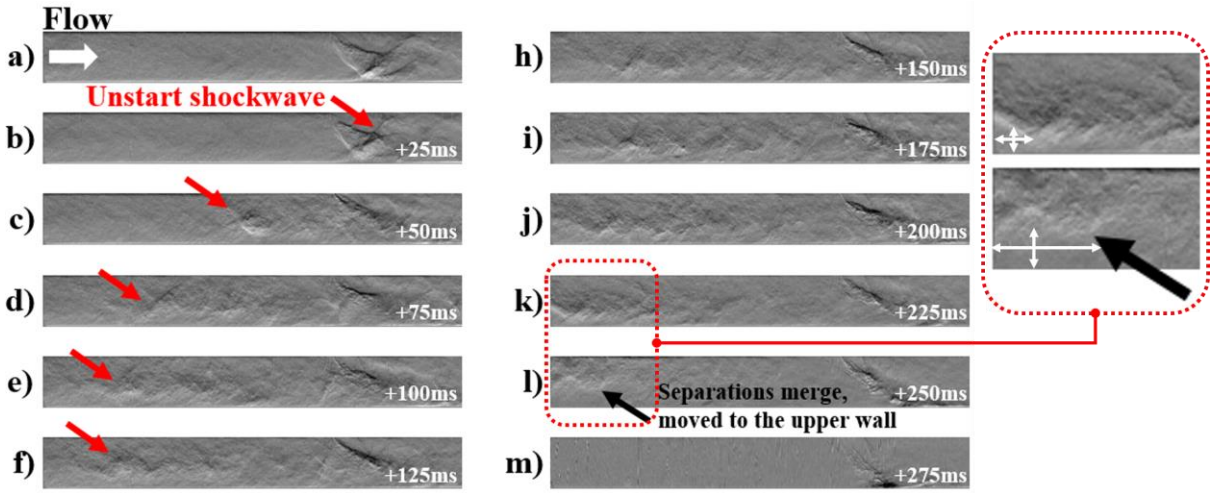

Fig. 10 Unstart shockwave propagation at the isolator

Figure 11 describes the rapid unstart shock disgorgement procedure from the inlet. Just before reaching the inlet, separations from the first shockwave impingement and the unstart shockwave merge, forming a larger single separation zone at the upper wall (See Fig. 10(l)). This merged separation zone greatly reduces the effective area of the flow and hence choked mass flow rate is reduced. Furthermore, there are no strong compression waves in the region upstream of the incident shockwave, except for the weak Mach wave originating from the cowl (lower lip of the inlet, above the images in Fig. 11), the unstart shock propagation gets even faster as it is driven by the strongest adverse pressure gradient, i.e., compression from the first shockwave impingement. It only takes less than 10ms (approximately 12 m/s which is the fastest among other regions) to completely disgorge the oblique shockwave system out of the inlet (Fig. 11(d)) from the first appearance of the unstart shock in the imaging section (Fig. 11(a)). After being unstarted, the inlet flow is known to be highly unsteady, however, the schlieren images look rather uniform (Fig. 11(d)) because the Mach number is significantly reduced due to a strong and unsteady shockwave staying in front of the inlet.

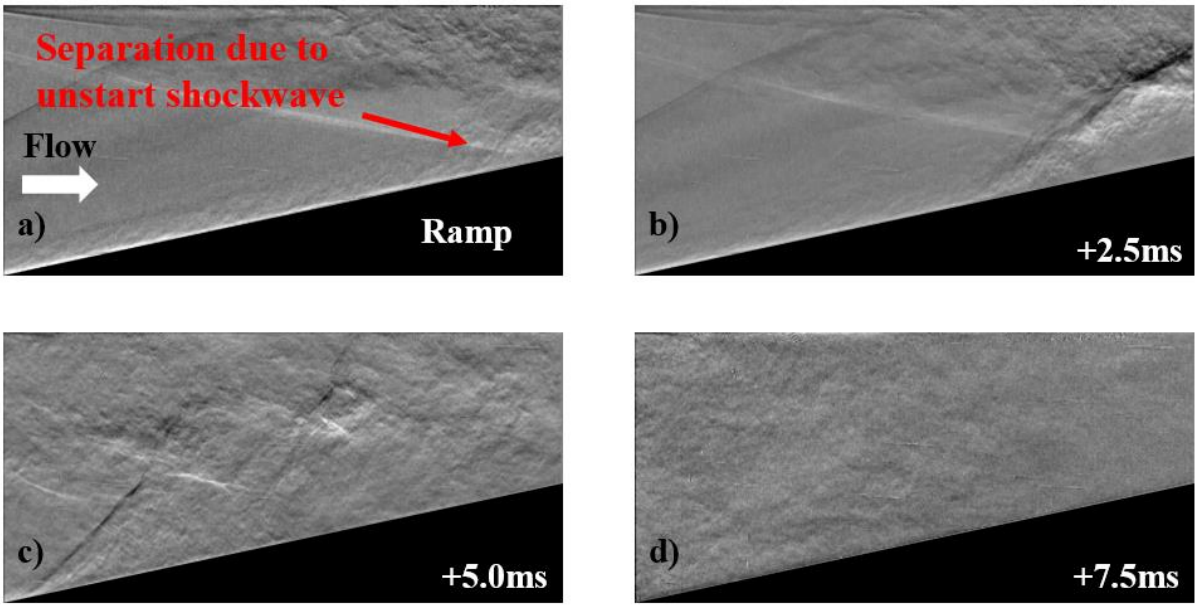

Fig. 11 Unstart shock propagation at the inlet

3.2. Case 2: Inlet unstart with boundary-layer suction, fast actuation

The unstarting flows through the inlet-isolator-combustor channel are visualized using schlieren imaging again under the identical flow conditions, but with the boundary layer suction activated at varied delays from the beginning of nitrogen jet injection. The delays are applied to ensure supersonic jet structures to be developed. In Case 2, the boundary layer suction is activated at 10ms after the nitrogen jet injection. The time-sequential schlieren images that are concatenated to show the flow region throughout the isolator and combustor are presented in Fig. 12. The overall flow structures and the detailed features are almost exactly identical to those seen without the boundary layer suction shown in Fig. 7 during the period from 25 ms to 100 ms time delays from the beginning of the tunnel run, hence these images are not presented in the figure. As the boundary layer suction is active, the unstart shock stops moving upstream and stays in the region of the suction holes. Later as the jet injection rate gradually decreases, the unstart shock moves downstream (Figs. 12(e) and 12(f)), and the inlet remains started (no flow spillage or shock disgorgement at the inlet) during the whole tunnel operation time. The suction pressure history is monitored to estimate the suction flow rate that turns out to be only approximately 1.9% of the freestream mass flow rate.

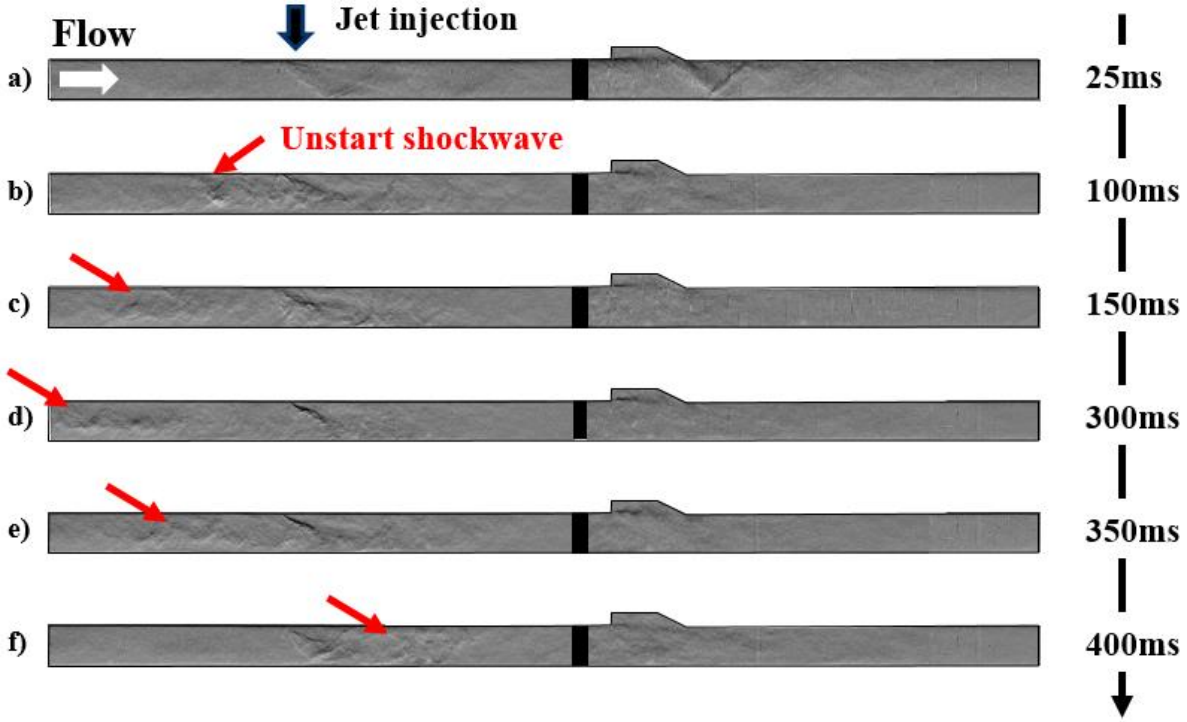

Fig. 12 Inlet unstart with suction (Case 2)

3.3. Case 3: Inlet unstart with boundary-layer suction, late actuation

In Case 3, the boundary layer suction is activated 20 ms after the beginning of the nitrogen jet injection. Figure 13 presents the temporal evolution of the flow structures in the model scramjet with the suction activated while the model scramjet undergoes the inlet unstart process. As in Case 2 (Fig. 12) with earlier boundary layer suction, and the Case 1 (Fig. 7) without the suction, the flow behavior is similar between 25 ms and 100 ms time delays. However, unlike in Case 2, the unstart shock continues to move further upstream, and eventually the inlet unstarts at 350 ms to make the downstream flow subsonic throughout (Fig. 13(g)). Interestingly, the maximum suction pressure is roughly 1.3 times greater than that in Case 2 although all other flow conditions are exactly the same, which corresponds to the boundary layer suction of 2% of the total flow rate.

This observation explicitly implies that the removal of 2% of the total mass flow is insufficient to make the inflow rate balanced with the outflow rate, and the mechanism stopping the unstart in Case 2 is not simply due to the reduction of mass flow rate via the boundary layer suction, even though unstart originates from the same mass imbalance. We conjecture that the earlier suction in Case 2 could effectively shut the downstream pressure propagation channel that is the subsonic core of the boundary layer. However, the later activation of the suction as in Case 3 might be too late to completely close the channel. For an instance, when the suction is activated at 20 ms after as in Case 3, the subsonic core of the boundary layer could have become too thick to be completely removed by the suction being limited by the hole size and the given pressure difference; recall that 20 ms is sufficiently long for the pressure waves originating from the high-pressure downstream region to reach the isolator entrance through the subsonic boundary layer core area. On the other hand, in Case 2, the unstart shock anchors at a location near the entrance of the isolator in steady-state which indicates that the inlet-captured inflow (roughly 98% due to the mass removal) is fully taken through the choked throat. In other words, the choked flow rate in Case 2 is greater than that in Case 3 since the inlet-captured inflow rate has not changed. This would be due to the enlarged effective core flow area in the isolator region which will result in a higher choked mass flow rate.

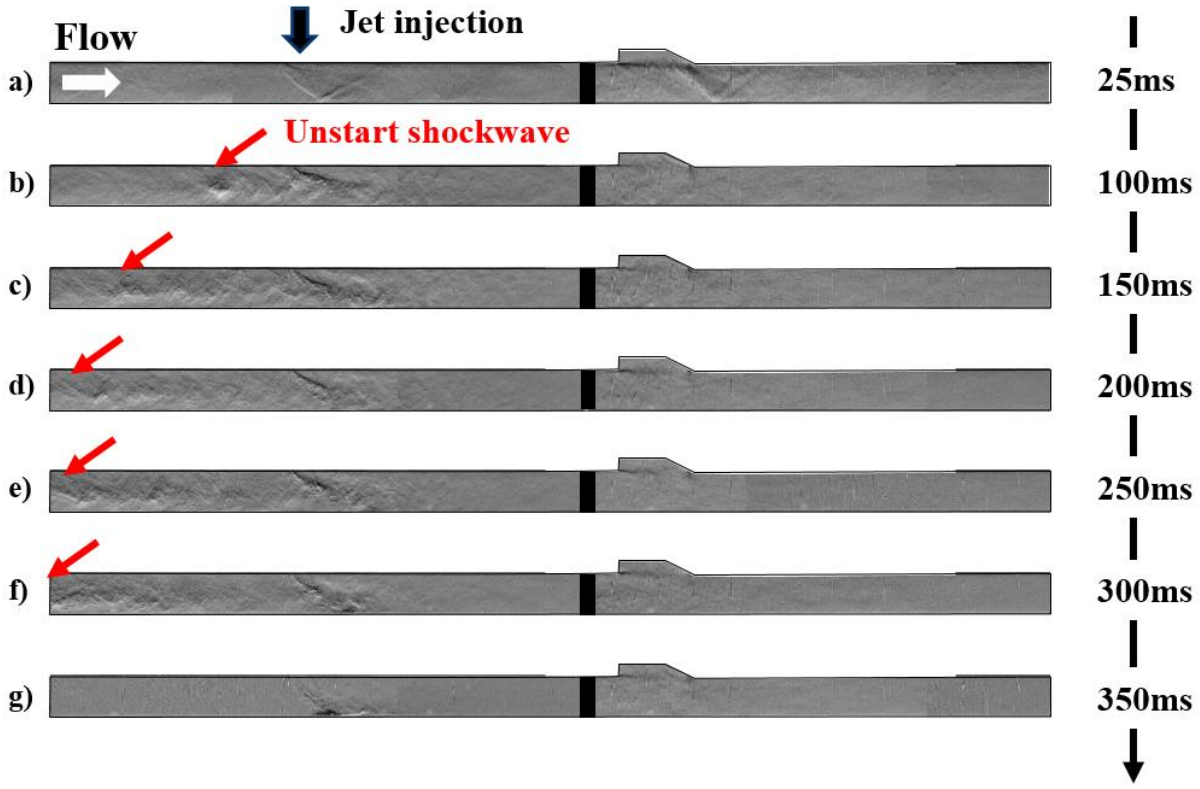

Fig. 13 Inlet unstart with suction (Case 3)

4. Conclusion

Scramjet inlet unstart process has been experimentally investigated using high-speed schlieren imaging of a model scramjet installed in a supersonic wind tunnel generating Mach 6 freestreams in an open-jet type test section. A high-pressure nitrogen jet was injected into the combustor area to cause downstream flow choking to trigger inlet unstart. A typical unstart shock system appeared downstream in the combustor and propagated upstream passing through the cavity flameholder, the high-pressure nitrogen jet, and the inlet. When the unstart shock reaches the inlet and causes flow spillage and strong shockwave formation in front of the inlet, the inlet-captured mass flow rate decreases to match the choked flow rate, which is referred as inlet unstart. The inlet unstart will result in a sudden drop of thrust, and induction of strong, unsteady, and asymmetric drag on the forebody of the scramjet vehicle and should be avoided actively in flight.

To prevent the inlet unstart, in the case where the unstart process has already been initiated by downstream flow choking, the upstream propagation of the unstart shock should be stopped prior to reaching the inlet area. It was found that the unstart shock propagation behavior is strongly dependent on the local pressure gradient and the stagnation pressure profile and the propagation speed varied from less than 1 m/s to slightly over 10 m/s. The shock propagation gets significantly decelerated as it moves upstream where the freestream speed and stagnation pressure are higher. To delay or stop the unstart shock propagation, suction with the perforated isolator wall was applied to suppress the boundary layer growth. It was found that the boundary layer suction was effective in increasing the effective area of the flow and removing the subsonic core of the boundary layer, both of which increase the choked mass flow rate. The subsonic core of the boundary layer serves as a channel for pressure waves originating from the high-pressure downstream region that expands the subsonic core and thickens or separates the boundary layers to result in flow deceleration and additional stagnation pressure loss.

The boundary layer suction (approximately 2% of the total mass flow was removed from the boundary layer) was activated 10ms and 20ms after the high-pressure nitrogen jet injection, respectively, to reveal the influence of actuation timing. The fast actuation (10 ms delay) could stop the shock propagation in steady-state, therefore, the inlet remained started during the whole tunnel operation time. Nevertheless, the late actuation (20 ms delay) could only delay the inlet unstart by tens of milliseconds, which can still help in saving time for activating other primary but slower control strategies such as the control of fuel injection rate. We conjecture that this discrepancy is because the late suction could not effectively remove the subsonic core of the boundary layer which grows in time: higher suction rate is required to suppress boundary layer as it gets thicker while the suction rate is limited in practice. In conclusion, it was confirmed that the boundary layer suction should be actuated early enough to be effective in stopping and preventing inlet unstart.

Acknowledgment

This work was supported by Basic Research Funding of Korean Agency for Defense Development (Project Number: 15-201-502-025).

Lydia Wermer was supported by US National Science Foundation Graduate Research Fellowship Program (Grant No.DGE11-6756).

- Journal article

1. SATO, TETSUYA, and SHOJIRO KAJI. "Study on steady and unsteady unstart phenomena due to compound choking and/or fluctuations in combustor of scramjet engines." 4th Symposium on Multidisciplinary Analysis and Optimization. 1992.
2. McDaniel, Keith, and Jack Edwards. "Simulation of thermal choking in a model scramjet combustor." 30th Fluid Dynamics Conference. 1999.
3. Mashio, Susumu, et al. "Unstart phenomenon due to thermal choke in scramjet module." 10th AIAA/NAL-NASDA-ISAS International Space Planes and Hypersonic Systems and Technologies Conference. 2001.
4. McDaniel, Keith, and Jack Edwards. "Three-dimensional simulation of thermal choking in a model scramjet combustor." 39th Aerospace Sciences Meeting and Exhibit. 2001.
5. Tan, Hui-jun, Shu Sun, and Zhi-Long Yin. "Oscillatory flows of rectangular hypersonic inlet unstart caused by downstream mass-flow choking." Journal of Propulsion and Power 25.1 (2009): 138-147.
6. Do, Hyungrok, et al. "Visualizing supersonic inlet duct unstart using planar laser Rayleigh scattering." Experiments in fluids 50.6 (2011): 1651-1657.
7. Qifan, Zhang, Tan Huijun, and Bu Huanxian. "Investigation of a Movable Slot-Plate Control Method for Hypersonic Inlet Unstart Caused by Downstream Mass-Flow Choking." 50th AIAA/ASME/SAE/ASEE Joint Propulsion Conference. 2014.
8. Holland, Scott D. "Wind-tunnel blockage and actuation systems test of a two-dimensional scramjet inlet unstart model at Mach 6." (1994).
9. Shimura, Takashi, et al. "Load oscillations caused by unstart of hypersonic wind tunnels and engines." Journal of Propulsion and Power 14.3 (1998): 348-353.
10. Liu, Qili, et al. "Ethylene flame dynamics and inlet unstart in a model scramjet." Journal of Propulsion and Power 30.6 (2014): 1577-1585.

11. Babinsky, Holger, Nick Makinson, and Claire Morgan. "Micro-vortex generator flow control for supersonic engine inlets." 45th AIAA Aerospace Sciences Meeting and Exhibit. 2007.
12. Babinsky, H., Yl Li, and C. W. Pitt Ford. "Microramp control of supersonic oblique shock-wave/boundary-layer interactions." AIAA journal 47.3 (2009): 668-675.
13. Valdivia, A., et al. "Control of supersonic inlet-isolator unstart using active and passive vortex generators." AIAA journal 52.6 (2014): 1207-1218.
14. Im, S., H. Do, and M. A. Cappelli. "The manipulation of an unstarting supersonic flow by plasma actuator." Journal of Physics D: Applied Physics 45.48 (2012): 485202.
15. Xing, Fei, et al. "Numerical investigation on shock train control and applications in a scramjet engine." Aerospace Science and Technology 60 (2017): 162-171.
16. Chang, J., et al. "Effects of boundary-layers bleeding on unstart/restart characteristics of hypersonic inlets." The Aeronautical Journal 113.1143 (2009): 319-327.
17. Fan, Y., et al. "Effects of boundary-layer bleeding on unstart oscillatory flow of hypersonic inlets." The Aeronautical Journal 114.1157 (2010): 445-450.
18. Kouchi, Toshinori, Tohru Mitani, and Goro Masuya. "Numerical simulations in scramjet combustion with boundary-layer bleeding." Journal of propulsion and power 21.4 (2005): 642-649.
19. Im, Seong-kyun, and Hyungrok Do. "Unstart phenomena induced by flow choking in scramjet inlet-isolators." Progress in Aerospace Sciences (2018).
20. Baccarella, D., et al. "Development and testing of the ACT-1 experimental facility for hypersonic combustion research." Measurement Science and Technology 27.4 (2016): 045902.
21. Do, Hyungrok, et al. "The influence of boundary layers on supersonic inlet flow unstart induced by mass injection." Experiments in fluids 51.3 (2011): 679.
22. Im, S., et al. "Unstart phenomena induced by mass addition and heat release in a model scramjet." Journal of Fluid Mechanics 797 (2016): 604-629.